SUPPLEMENTARY MATERIAL

Determination of hydroquinone and benzoquinone in pharmaceutical formulations: critical considerations on quantitative analysis of easily oxidized compounds

Olívia Brito de Oliveira Moreira[a], Lucas Vinicius de Faria[a], Renato Camargo Matos[a], Karine Braga Enes[a], Mara Rúbia Costa Curi[a], Marcone Augusto Leal de Oliveira[a,b].

[a]*Chemistry Department, Institute of Exact Sciences, Federal University of Juiz de Fora, 36026-900, Juiz de Fora, MG, Brazil.*

[b]*National Institute of Science and Technology for Bioanalytics – INCTBio, Institute of Chemistry, University of Campinas (UNICAMP), 13083-970, Campinas, SP, Brazil*

Corresponding author: marcone.oliveira@ufjf.br

1. Solid-state NMR

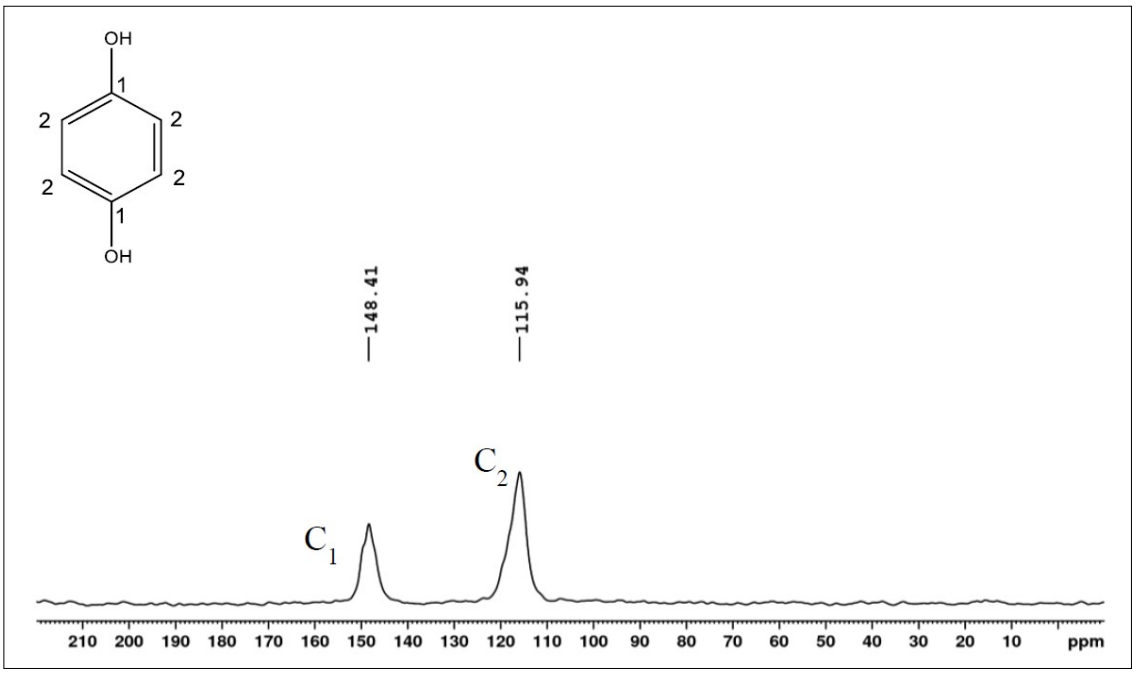

Fig. 1S. Solid-state ^{13}C NMR of the hydroquinone standard material.

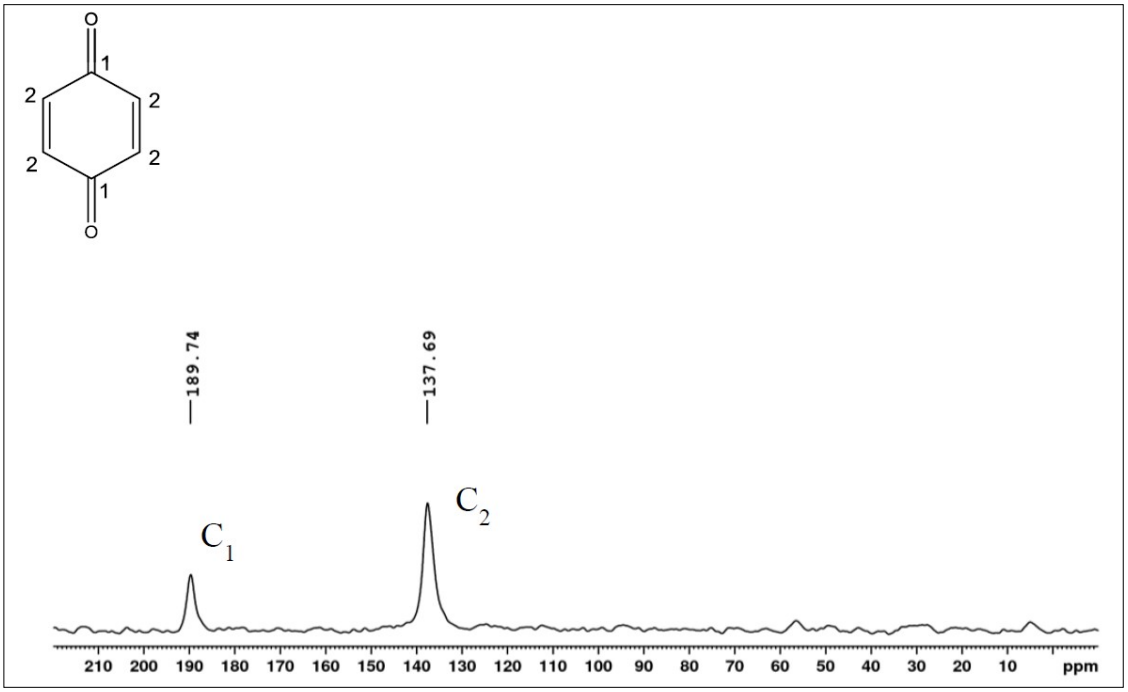

Fig. 2S. Solid-state ^{13}C NMR of the benzoquinone standard material.

2. FT-IR and Raman

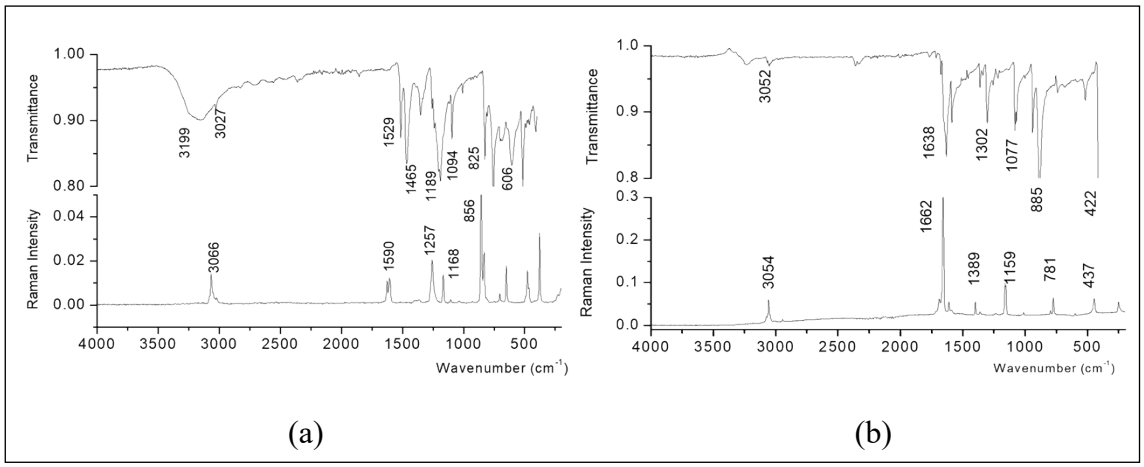

Fig. 3S. FT-IR and Raman spectra of (a) HQ and (b) BQ. Experimental conditions FT-IR: 54 scans with 4 cm^{-1} of resolution; Raman: 10 mW of power, 512 *scans* with 4 cm^{-1} of resolution.

Table 1S. Characterization of vibrational spectra of HQ and BQ for both FT-IR and Raman scattering

Bond type	Hydroquinone		Benzoquinone	
	IR	RAMAN	IR	RAMAN
ν(O-H)	3199	-	-	-
ν(C-H)	3027	3066	3052	3054
ν(C=O)	-	-	1662	1683
ν(C=C)	1529	1590	1302	1389
δ(O-H)	1465	-	-	-
ν(C-O)	1189	1227	-	-
β(C-H)	1094	1168	-	-
γ(C-H)	825	856	885	781
τ(O-H)	606	-	-	-
β (C=O)	-	-	422	437

ν = stretching; δ = in-plane symmetric deformation; β = in-plane asymmetric deformation; γ = out-of-plane bending τ = out-of-plane bending (twisting).

3. NMR of HQ and BQ deuterated solutions

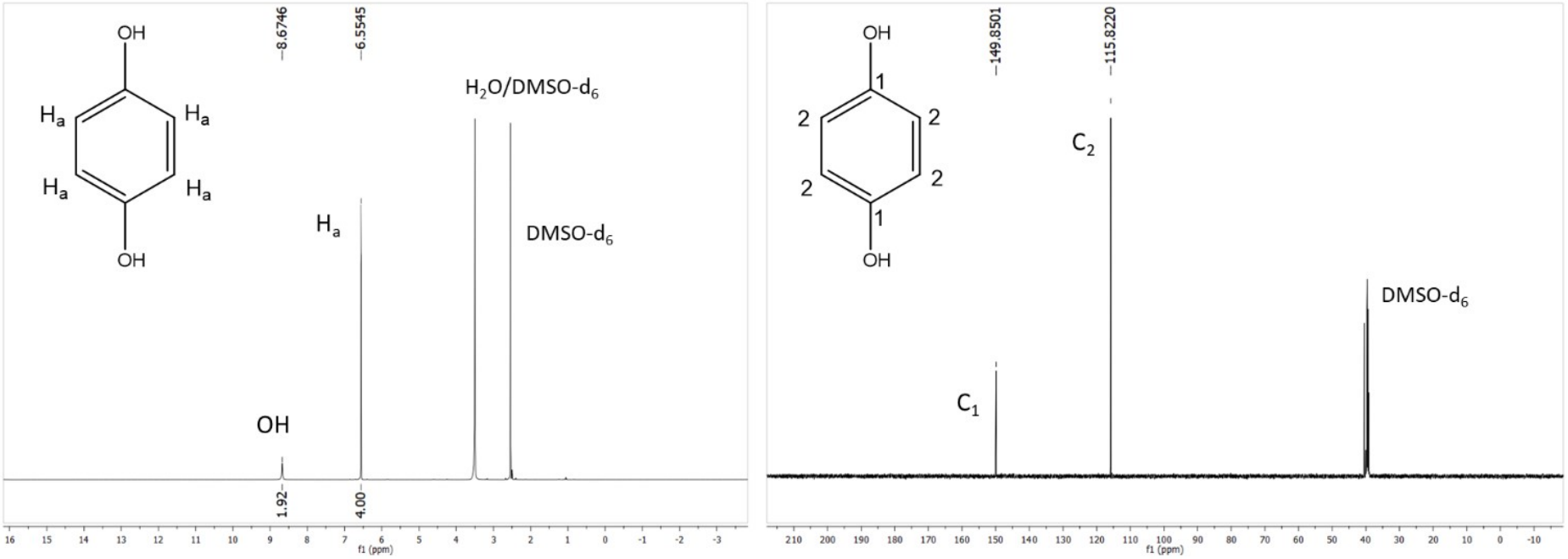

Fig 4S. ^{1}H and ^{13}C NMR of hydroquinone in DMSO-d_6.

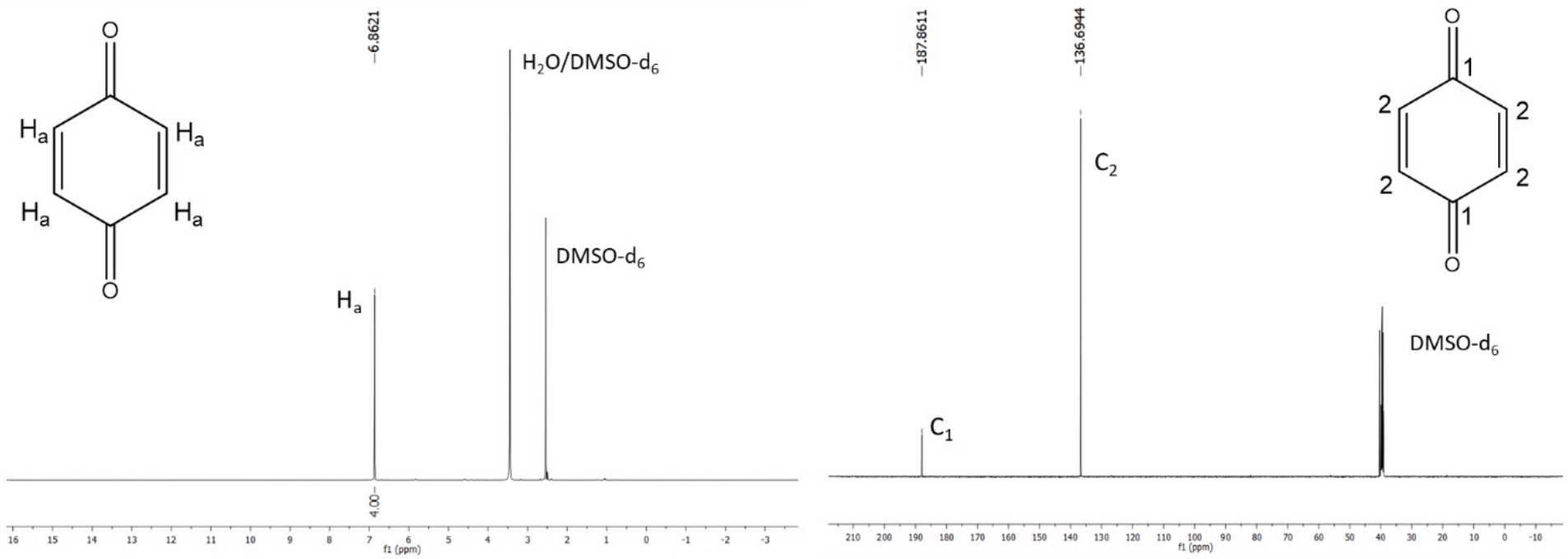

Fig 5S. ^{1}H and ^{13}C NMR of benzoquinone in DMSO-d_6.

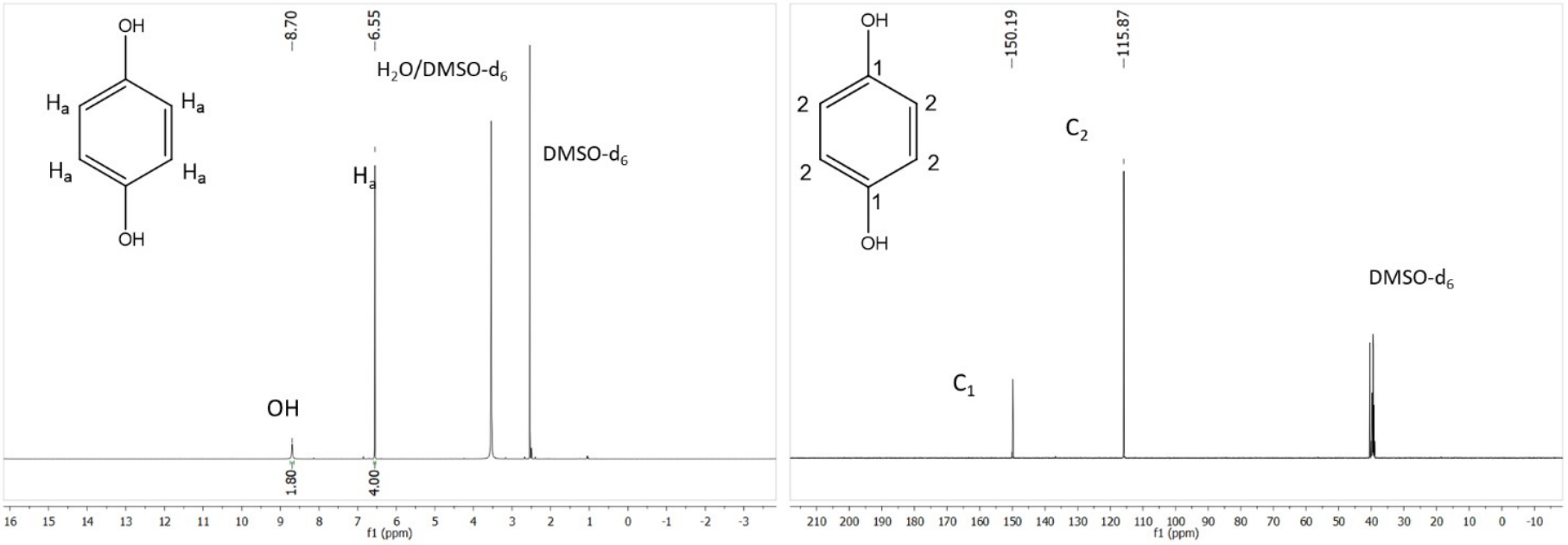

Fig 6S. ^{1}H and ^{13}C NMR of hydroquinone in DMSO-d_6 after a week from the preparation date.

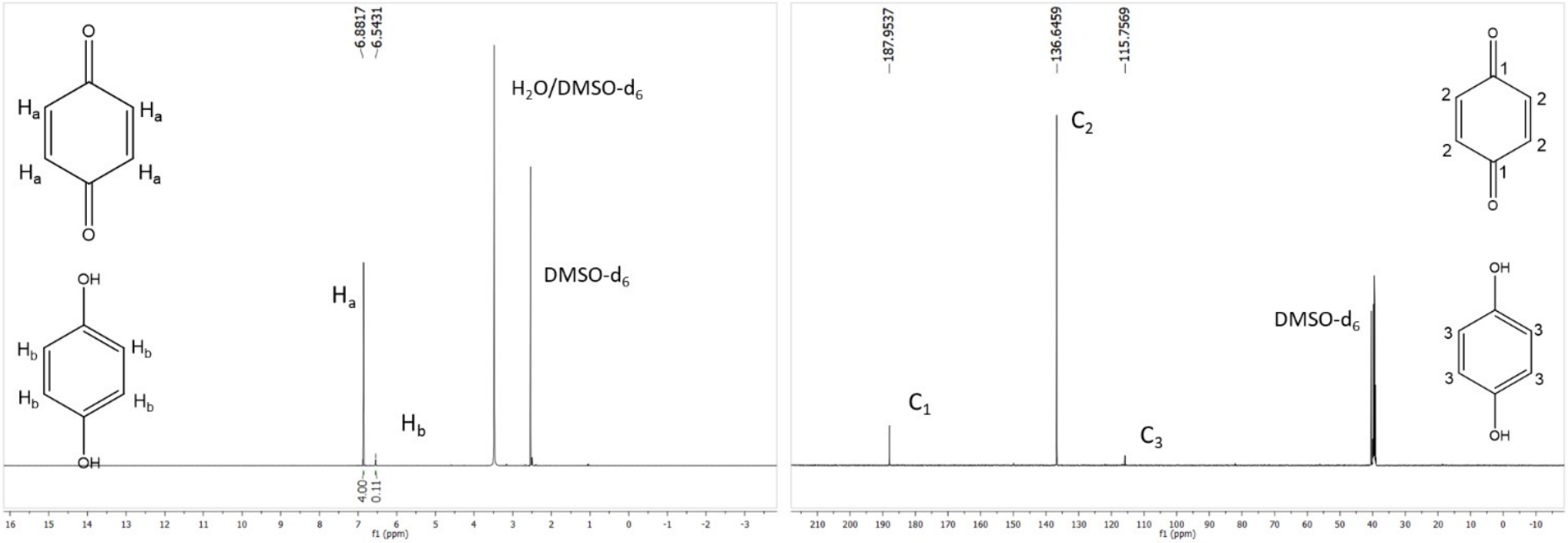

Fig 7S. ^{1}H and ^{13}C NMR of benzoquinone original tube in DMSO-d_6 after a week from the preparation date.

4. Raman scattering of samples and standards

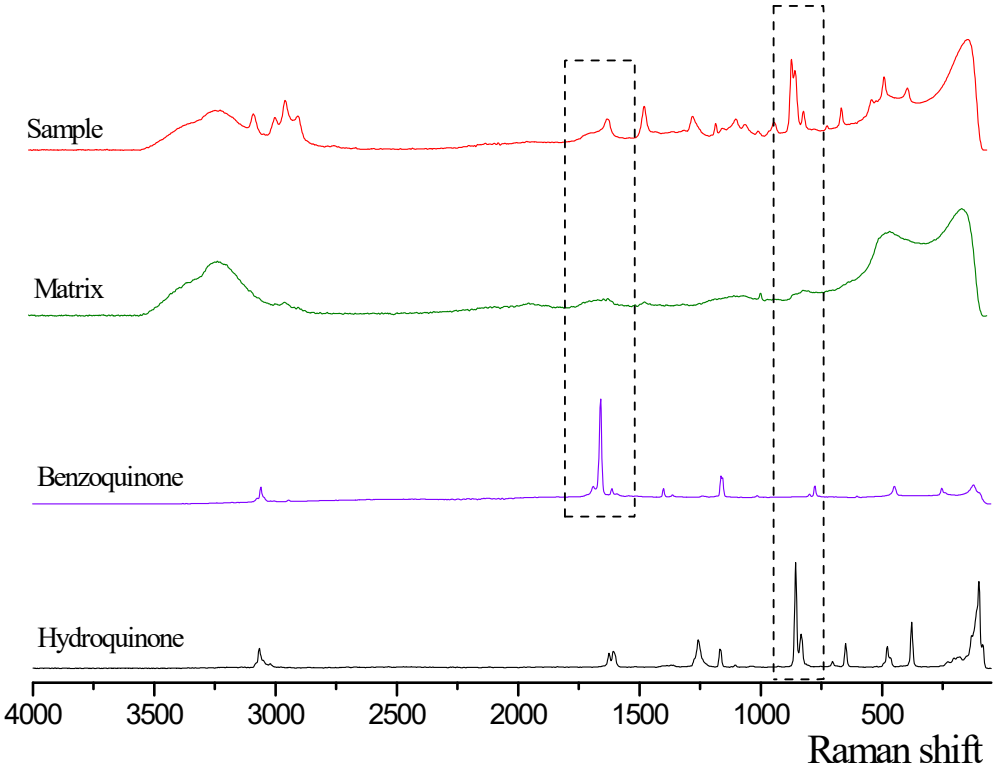

Fig 8S. Comparative analysis of Raman Scattering spectra of a HQ-based pharmaceutical sample, the sample matrix, HQ and BQ standard crystals. Power of excitation source: 10 mW for HQ and BQ, 100 mW for sample and matrix. 512 scans. 4 cm^{-1} resolution.

5. E(V) *vs* pH curves

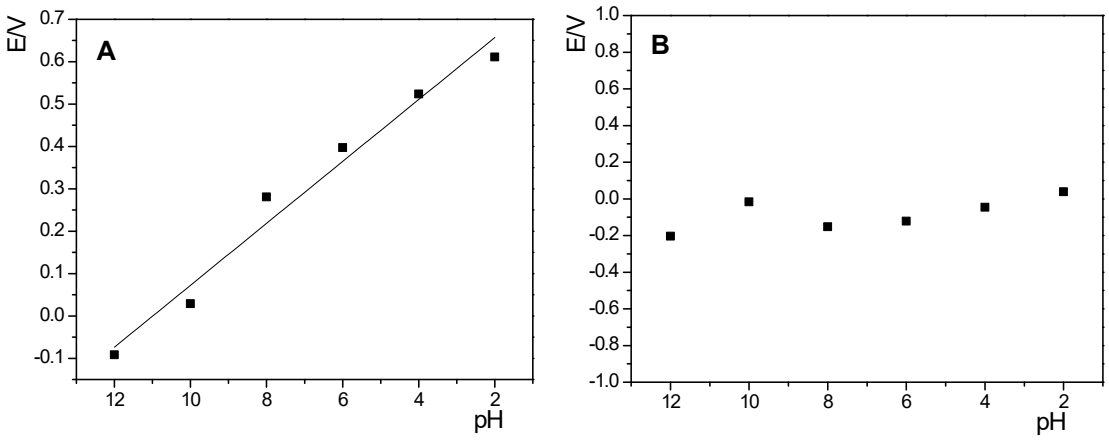

(a) (b)

Fig 9S. E(V) *vs* pH curve of (A) HQ oxidation peak potentials and (B) BQ reduction peak potentials.

6. Distribution diagram

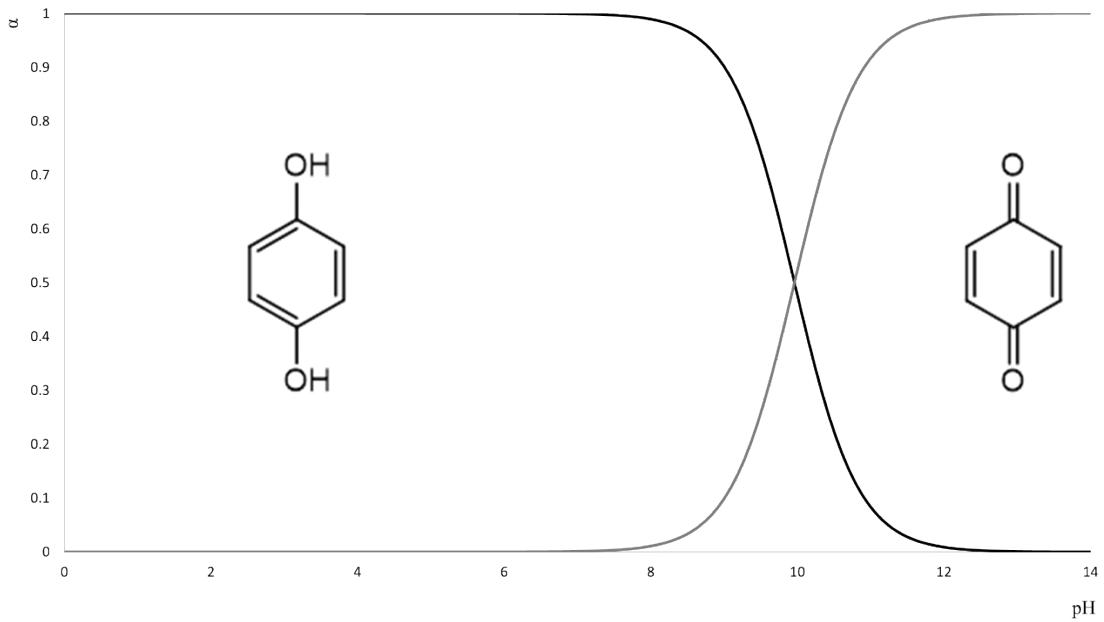

Fig. 10S. Distribution diagram of HQ/BQ along the pH scale.

7. Visual indicatives of hydroquinone oxidation

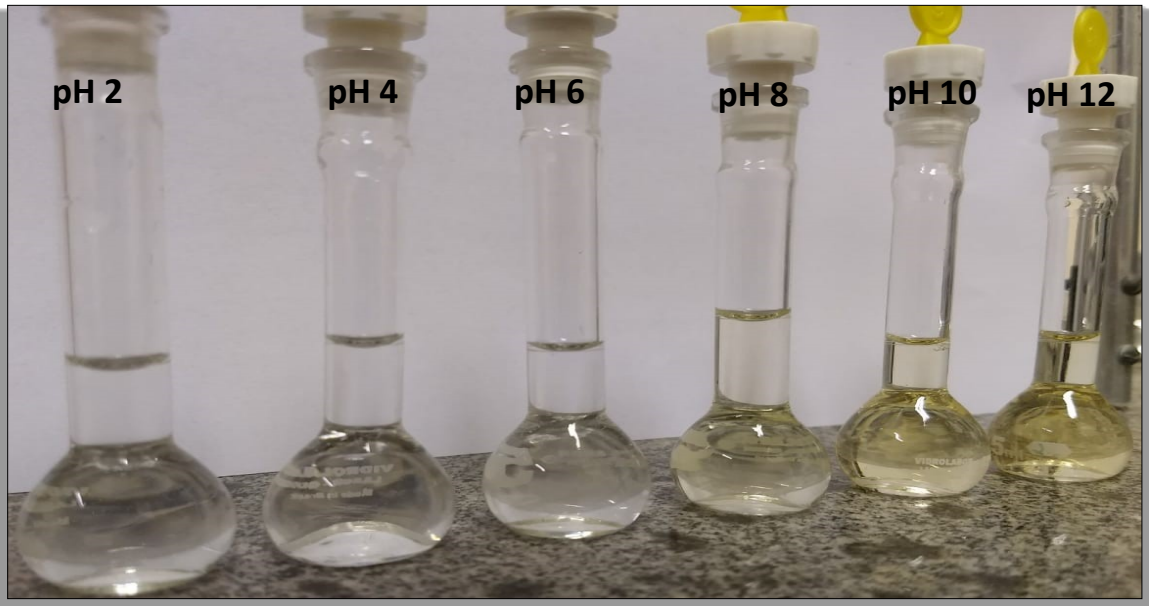

Fig.11S**.** Modification on the color of aqueous solution of HQ according to the pH scale.

8. Micellar Electrokinetic Chromatography (MEKC) experiments

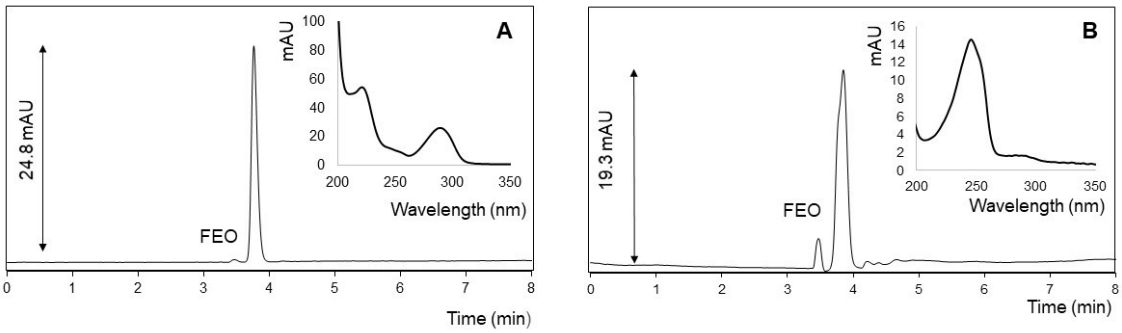

Fig 12S. Electropherograms of 10 mmol L^{-1} HQ in water/methanol (9:1, *v/v*). Electrophoretic conditions: 25 ºC, +2 0 kV, hydrodynamic injection: 50 mbar for 5 s, detection at 287 nm (**A**) and 248 nm (**B**). 48.5 cm (40 cm effective length) and 75 µm i.d. capillary. BGE: 20 mmol L^{-1} Tris/Phosphate buffer (pH 7.5), 40 mmol L^{-1} SDS and 10 % (*v/v*) acetonitrile. UV spectra was acquired by the DAD detector.

The expected for a MEKC analysis of HQ were a single peak associated to the HQ UV spectrum. However, since the experiment was set up to run in both HQ and BQ maximum wavelengths (287 and 248 nm respectively), it had allowed us to notice an indicative of oxidation, once the UV spectrum acquired in 248 nm is characteristic of the BQ structure.

9. Determination of diffusion coefficient (D)

The active area of the glassy carbon working electrode used in all experiments was calculated from a solution of known diffusion coefficient, and in this case we selected potassium ferricyanide probe ($K_3Fe(CN)_6$) as the model molecule. Subsequently an aliquot of 1 mmol L^{-1} of the probe was added to the electrochemical cell containing KCl 100 mmoL^{-1} as the supporting electrolyte and CV measurements under the potential range of -0.2 to 0.7 V using scan rate ranging from 25 to 300 mV s^{-1} were performed.

With the data collected from the resulting voltammograms, the linear regression that relates current i_p (µA) and $v^{1/2}$ (Vs^{-1}) was calculated so the slope along with the other parameters related to Fe (III) would be used in the Randles-Sevcik equation to finally get the electrode area. Following this protocol, a value of 0.060 cm^2 was found.

i_p (μA) *versus* $v^{1/2}$ linear regression was prepared using both HQ and BQ solutions. The analysis followed the same protocol above mentioned. The standard solutions were individually added to the electrochemical cell containing BR buffer at pH 7 and CV measurements under the potential range of (-0.7 V to 0.9 V for HQ and 0.9 V to -0.7 V for BQ) using scan rate ranging from 25 to 300 mV s^{-1} were carried out. The individually calculated slopes of i_p (μA) *versus* $v^{1/2}$ (Vs^{-1}) equation together with the working electrode area previously calculated were finally used to calculate the diffusion coefficient of each analyte also through the Randles-Sevcik equation.

10. Chronoamperometric analysis of benzoquinone: limit of detection

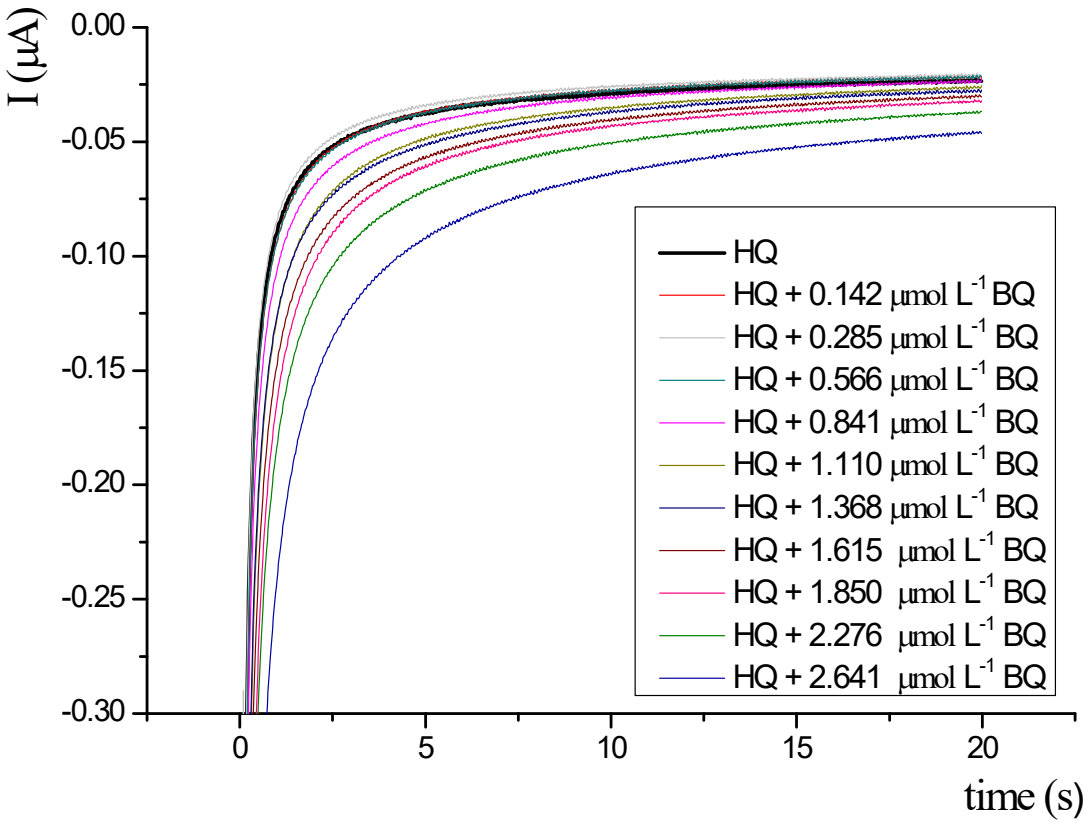

Fig 13S. Chronoamperometric analysis of addition of benzoquinone aliquots to a hydroquinone solution. Supporting electrolyte: BR buffer (0.04 mol L^{-1}, pH 5.5). Glassy-carbon working electrode, $Ag/AgCl_{(sat)}$ reference electrode and platinum auxiliary electrode. Potential applied: -0.1 V.

11. Optimization of extraction solvent for sample preparation

Table 2S. Comparative evaluation of hydroquinone assay results in dermatological gel in samples prepared with and without the addition of 10 % methanol.

Diluent A: BR buffer (pH 5.5)		Diluent B: BR buffer (pH 5.5) and methanol (9:1, *v/v*)	
[HQ] (%, *w/w*)	2.91	[HQ] (%, *w/w*)	3.81 %
RSD (%)	2.09	RSD	0.21 %

n = 3

RSD (%) = Relative Standard Deviation, calculated through the ratio between the standard deviation and the average of all measurements.

12. Selectivity test

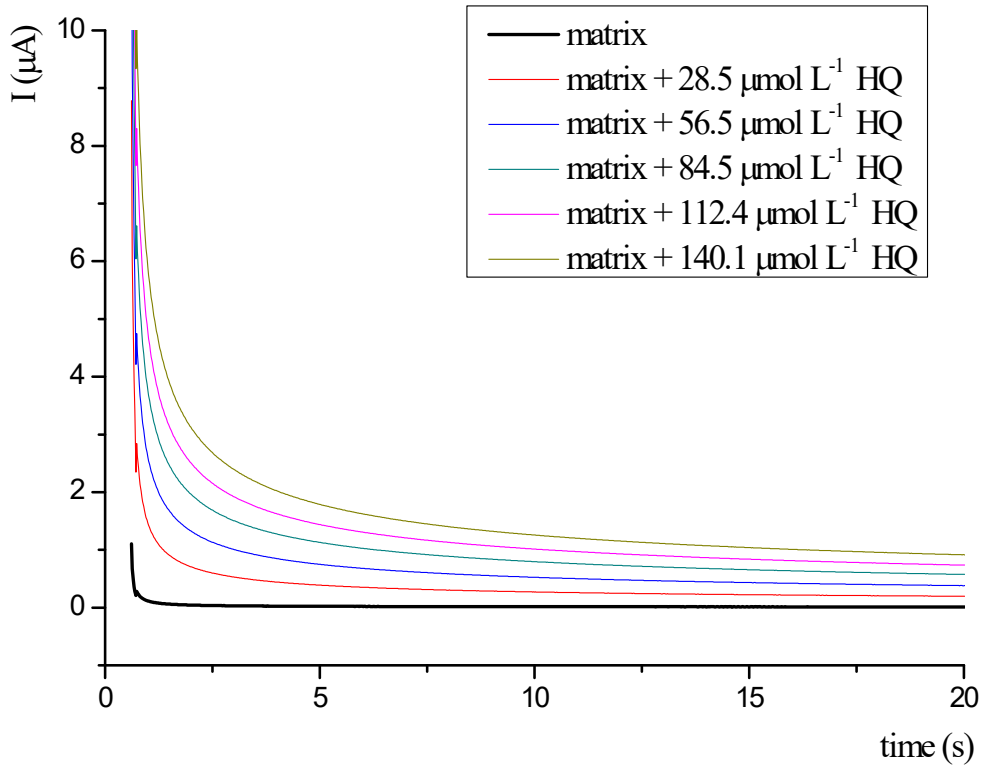

Fig 14S. Selectivity test carried out by the optimized chronoamperometric method. Supporting electrolyte: BR buffer (0.04 mol L^{-1}, pH 5.5). Glassy-carbon working electrode, $Ag/AgCl_{(sat)}$ reference electrode and platinum auxiliary electrode. Potential applied: 0.4 V. Scan rate: 100 mVs^{-1}.

13. Oxidation traceability of the HQ pharmaceutical sample

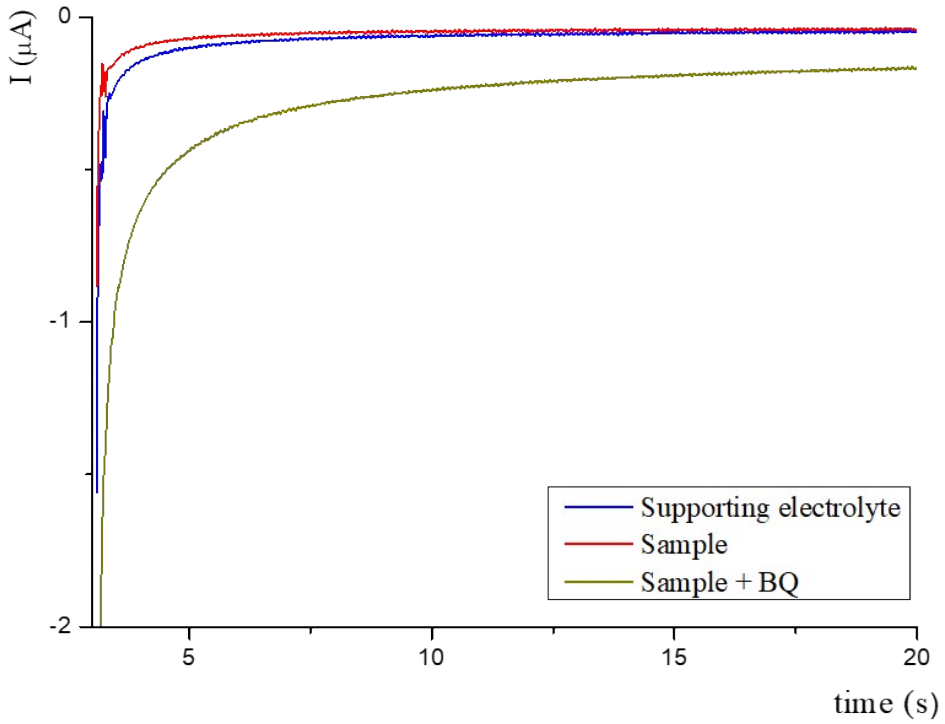

Fig 15S. Chronoamperogram resulting from the application of reduction potential on the dermatological gel sample containing hydroquinone. Supporting electrolyte: BR buffer (0.04 mol L^{-1}, pH 5.5). Glassy-carbon working electrode, $Ag/AgCl_{(sat)}$ reference electrode and platinum auxiliary electrode. Potential applied: -0.1 V.